J Solution Chem (2015) 44:1963–1975
DOI 10.1007/s10953-015-0377-2

Measurements and Calculations of the Solid–Liquid Equilibria in the Quaternary Systems NaBr–KBr–$MgBr_2$–H_2O and NaBr–KBr–$CaBr_2$–H_2O at 348.15 K

Juanxin Hu[1,2] · **Shihua Sang**[1,2] · **Qingzhu Liu**[1,2]

Received: 2 January 2015 / Accepted: 25 April 2015 / Published online: 1 October 2015

Abstract Solid–liquid equilibria in the quaternary systems NaBr–KBr–$MgBr_2$–H_2O and KBr–NaBr–$CaBr_2$–H_2O at 348.15 K were determined using the method of isothermal solution saturation. The solubilities of the equilibrium solutions were determined. According to the experimental data, the equilibrium phase diagrams and water content diagrams of the two quaternary systems were plotted. The solubility diagram of the quaternary NaBr–KBr–$MgBr_2$–H_2O system has two invariant points, five univariant curves, and four crystallization fields (which are saturated with $MgBr_2{\cdot}6H_2O$, $KBr{\cdot}MgBr_2{\cdot}6H_2O$, NaBr and KBr, respectively, where $KBr{\cdot}MgBr_2{\cdot}6H_2O$ is a double salt). The solubility diagram of the quaternary system KBr–NaBr–$CaBr_2$–H_2O includes one invariant point, three univariant curves, and three crystallization fields ($CaBr_2{\cdot}2H_2O$, KBr and NaBr). The dissolution equilibrium constant K of NaBr, KBr, $MgBr_2{\cdot}6H_2O$, $KBr{\cdot}MgBr_2{\cdot}6H_2O$ and $CaBr_2{\cdot}2H_2O$ at 348.15 K were fitted using Pitzer's equation. A chemical model based on the Pitzer equation was constructed to calculate the solubilities of salts in the two quaternary systems at 348.15 K. The calculated solubilities are in agreement with experimental results.

Keywords Solid–liquid equilibrium · Pitzer model · Solubility · Bromide salts

1 Introduction

The studies of phase equilibria in multicomponent salt–water systems at different temperatures are fundamental for the development and utilization of brine resources. Bromide rich brines are widely distributed in the Qinghai–Tibet plateau and the Sichuan basin in

---

✉ Shihua Sang
sangsh@cdut.edu.cn; shihuasang@126.com

[1] College of Materials, Chemistry and Chemical Engineering, Chengdu University of Technology, Chengdu 610059, People's Republic of China

[2] Key Laboratory of Mineral Resources Chemistry for the Universities in Sichuan Province, Chengdu 610059, People's Republic of China

China. In recent decades, some scholars have investigated the phase equilibria of parts of the salt–water systems [1, 2]. In particular, the underground brines in the western Sichuan basin contain very abundant liquid mineral resources. The contents of boron, potassium, and bromine in these brines are far above the grades necessary for industrial utilization [3, 4]. The underground brines have stable chemical properties, and have high concentrations of potassium, sodium, boron, bromine, as well as accompanying lithium, strontium, magnesium, calcium, and many other useful components.

Underground brines are very complex salt–water systems, whose formation often involve solid–liquid equilibria. Furthermore, the phase diagrams at different temperatures play an important role in exploiting the brine resources and understanding the geochemical behavior of these brine–mineral systems. Therefore, it is necessary and urgent to investigate the thermodynamics (especially the phase equilibrium properties) of Br-rich brine–mineral systems at multiple temperatures.

A number of experimental and modelling studies on brine–salt mineral system have been carried out in recent decades. Aiming at the seawater system, Harvie et al. [5–8] carried out research into the prediction of mineral solubilities in natural waters of the Na–K–Mg–Ca–H–Cl–SO_4–OH–HCO_3–CO_3–CO_2–H_2O systems from zero to high concentration and as a function of temperature using Pitzer's equation. Felmy and Weare [9] predicted the borate mineral equilibria in Searles salt lake in the USA. In view of the abundant bromide resource in potash salt deposits, the phase equilibria and phase diagrams of the ternary KCl–KBr–H_2O system was determined at 298, 313, 333, 323 and 373 K, and the LiI–LiBr–H_2O and NH_4Br–LiBr–H_2O systems at 298 K [10–13]. In our previous work, we reported the phase diagrams of some bromide-rich ternary and quaternary systems, i.e., $K_2B_4O_7$–KBr–H_2O and $Na_2B_4O_7$–NaBr–H_2O at 298 K [14, 15], Na–K–Br–SO_4–H_2O at 323 K [16], NaCl–NaBr–Na_2SO_4–H_2O at 348 K [17], $Na_2B_4O_7$–NaBr–Na_2SO_4–H_2O at 348 K [18], and KCl–KBr–K_2SO_4 at 323 K [19].

Recently, Christov reported predictions of the solubilities of bromide salts and solution behavior in solid–liquid equilibrium systems [20–24]. The thermodynamic modeling was carried out to high concentration and temperature with Pitzer's equation. Due to the lack of solubility data involving bromide salts at different temperatures, the calculations were mainly focused on binary and ternary systems such as $CaBr_2$–H_2O, $MgBr_2$–H_2O, NaBr–H_2O, KBr–H_2O, NaBr–KBr–H_2O, NaBr–Na_2SO_4–H_2O, and KBr–K_2SO_4–H_2O [20–24].

Therefore, this paper has three objectives: (1) measure the solubilities of salts in the aqueous solutions of the quaternary systems NaBr–KBr–$CaBr_2$–H_2O and NaBr–KBr–$CaBr_2$–H_2O at 348.15 K, identify the equilibrium solid phases and construct the experimental phase diagrams and water content diagrams of the two quaternary systems; (2) use Pitzer's equation to fit the dissolution equilibrium constant of salts; and (3) use these thermodynamic data to develop a thermodynamic model for the prediction of bromide salt solubilities in the two quaternary systems.

2 Experimental Sections

2.1 Reagents and Instruments

Distilled water with conductivity less than 10^{-4} S·m^{-1} and pH = 6.6 was used for the phase equilibrium experiments and chemical analysis of samples. A HZ–9613Y type thermostated shaker with a precision ±0.1 K was used in the solid–liquid equilibrium measurements. NaBr, 99.0 % pure, was from Tianjin Zhiyuan Chemical Reagent Factory, China; $MgBr_2·6H_2O$ and $CaBr_2·2H_2O$, 98 % pure, were from Shanghai Xinbao Fine Chemical Plant, China; KBr, 99.0 % pure, was from the Chengdu area of the industrial development zone, Xindu Mulan, China.

2.2 Experimental Methods

The experiments were conducted by the method of isothermal solution saturation. Samples of the quaternary systems were prepared by gradual addition of the third salt to the saturated solution of the ternary subsystems at 348.15 K. The solid reagents and water were prepared in 100 mL glass bottles. Then, all bottles were sealed and placed in the thermostated shaker. The solid–liquid mixtures in the bottles were agitated for 1 week to accelerate equilibration. Experimental results show that equilibrium can be attained in 10–15 days under continuous shaking, and the time for the clarification of an aqueous solution is about 4–6 days. The clarified solutions were taken out periodically for chemical analysis. If the solution composition did not change, the system can be considered to have reached thermodynamic equilibrium. In this state, the solution composition should represent that of the saturated solution. Liquid samples were then taken for chemical analysis.

2.3 Analytical Methods

The concentration of K^+ was obtained by a gravimetric method using sodium tetraphenylborate (uncertainty: 0.5 %). The concentration of Mg^{2+} was determined by titration with an EDTA standard solution in the presence of the indicator eriochrome black T; an ammonium chloride buffer solution was used to maintain the high pH (10–11) of solutions in the complexometric titration process (uncertainty, 0.3 %). The concentration of Ca^{2+} was determined by titration with a standard EDTA solution in the presence of the indicator eriochrome K–B, while a sodium hydroxide solution was used for maintaining the high pH (11–12) of solutions in the complexometric titration (uncertainty: 0.5 %). The concentration of Br^- was measured by titration with silver nitrate solution (the Mohr method, uncertainty: ±0.3 %). The concentration of Na^+ was evaluated according to the charge balance of ions. The details of the above analytical methods can be found in the literature [25].

3 Results and Discussions

3.1 The $KBr–NaBr–MgBr_2–H_2O$ System

The experimental solubilities of salts in the quaternary system $KBr–NaBr–MgBr_2–H_2O$ at 348.15 K are given in Table 1. According to the solubilities, the corresponding dry salt compositions were calculated and are also tabulated in Table 1. Based on the dry salt composition, the phase diagram and water content diagram are presented in Figs. 1 and 2, respectively.

It can be seen from Table 1 and Fig. 1 that the double salt ($KBr·MgBr_2·6H_2O$) is formed in the quaternary system. The phase diagram (Fig. 1) is comprised of five

Table 1 Solubilities in the quaternary system NaBr–KBr–$MgBr_2$–H_2O at 348.15 K

No.	Composition of solution, *w* (%)[a]			Composition of dry salt *J* (g/100 g.S) *J* (NaBr + KBr + $MgBr_2$) = 100 g				Equilibrium solid[b]
	NaBr	KBr	$MgBr_2$	NaBr	KBr	$MgBr_2$	H_2O	
1, A_1	48.23	11.83	0	80.30	19.70	0.00	66.50	NB + KB
2	46.58	11.57	3.09	76.06	18.89	5.05	63.29	NB + KB
3	43.77	11.32	4.67	73.24	18.94	7.81	67.34	NB + KB
4	41.84	11.14	6.79	70.00	18.64	11.36	67.31	NB + KB
5	36.78	10.62	11.57	62.37	18.01	19.62	69.58	NB + KB
6	33.84	10.28	13.05	59.19	17.98	22.83	74.92	NB + KB
7	27.34	9.25	15.76	52.23	17.67	30.11	91.02	NB + KB
8	24.15	9.04	17.81	47.35	17.73	34.92	96.08	NB + KB
9	17.79	7.95	21.48	37.67	16.84	45.49	111.77	NB + KB
10	13.26	7.34	24.33	29.51	16.34	54.15	122.57	NB + KB
11	8.87	6.39	28.86	20.10	14.48	65.41	126.65	NB + KB
12, E_1	7.22	5.93	30.77	16.44	13.50	70.06	127.69	NB + KB + Car(Br)
13	7.12	5.73	30.72	16.34	13.15	70.51	129.52	NB + Car(Br)
14	6.83	5.38	33.35	14.99	11.81	73.20	119.49	NB + Car(Br)
15	5.46	4.43	35.27	12.09	9.81	78.10	121.43	NB + Car(Br)
16	4.81	3.71	38.4	10.25	7.91	81.84	113.13	NB + Car(Br)
17	4.19	2.37	41.2	8.77	4.96	86.26	109.38	NB + Car(Br)
18, F_1	3.11	1.46	43.3	6.50	3.05	90.45	108.90	NB + MB + Car(Br)
19	4.41	1.22	44.28	8.84	2.44	88.72	100.36	NB + MB
20	5.32	1.01	46.87	10.00	1.90	88.10	87.97	NB + MB
21	6.04	0.43	47.04	11.29	0.80	87.91	86.88	NB + MB
22, D_1	9.28	0	48.21	16.14	0.00	83.86	73.94	NB + MB
23	7.27	7.04	29.8	16.48	15.96	67.56	126.71	KB + Car(Br)
24	6.15	6.76	31.03	14.00	15.38	70.62	127.58	KB + Car(Br)
25	3.85	5.42	35.12	8.67	12.21	79.12	125.28	KB + Car(Br)
26	1.7	4.92	37.76	3.83	11.09	85.08	125.33	KB + Car(Br)
27, B_1	0	4.17	40.43	0.00	9.35	90.65	124.22	KB + Car(Br)
28	3.13	1.45	47.81	5.97	2.77	91.26	90.88	Car(Br) + KB
29	2.79	1.56	47.84	5.35	2.99	91.67	91.61	Car(Br) + KB
30, C_1	0	1.62	52.27	0.00	3.01	96.99	85.56	Car(Br) + MB

[a] *w* (%): mass% fraction

[b] NB, NaBr; KB, KBr; MB, $MgBr_2{\cdot}6H_2O$; Car(Br), $KBr{\cdot}MgBr_2{\cdot}6H_2O$

univariant curves (A_1E_1, E_1F_1, B_1E_1, C_1F_1 and D_1F_1) and two co-saturated points (E_1 and F_1). The four crystallization fields are $MgBr_2{\cdot}6H_2O$, $KBr{\cdot}MgBr_2{\cdot}6H_2O$, NaBr and KBr, respectively. The crystallization field of $MgBr_2{\cdot}6H_2O$ is smaller, which indicates that its solubility is greater in this system. The experimental results show that $MgBr_2$ has a strong salting-out effect on KBr and NaBr.

Figure 2 shows the water content diagram of the quaternary system KBr–NaBr–$MgBr_2$–H_2O at 348.15 K and the abscissa is the Jänecke index of *J* (KBr). Figure 2 shows that the

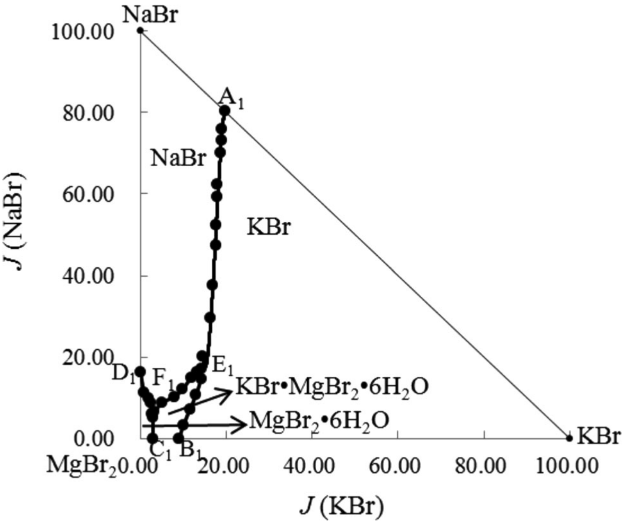

Fig. 1 Dry-salt solubility diagram of the quaternary system NaBr–KBr–$MgBr_2$–H_2O at 348.15 K

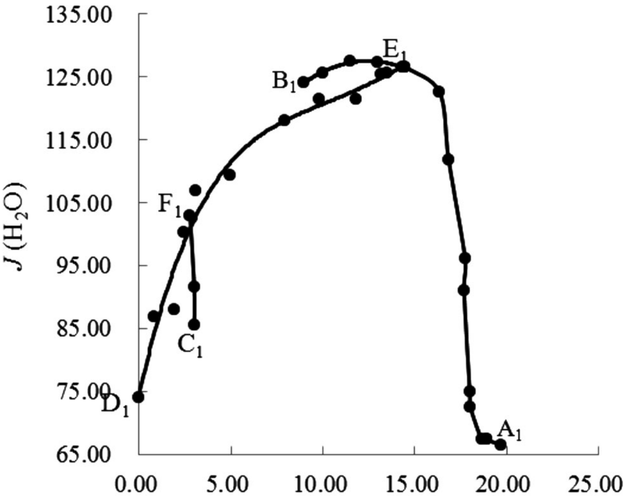

Fig. 2 Water contents of saturated solutions in the quaternary system NaBr–KBr–$MgBr_2$–H_2O at 348.15 K

water content increases at the univariant curves D_1F_1, and decrease at the univariant curves A_1E_1 with an increase of the Jänecke index values of *J* (KBr).

3.2 The KBr–NaBr–$CaBr_2$–H_2O System

The measured values of salt solubilities of the quaternary system KBr–NaBr–$CaBr_2$–H_2O at 348.15 K are presented in Table 2, where ion concentrations are expressed in mass

Table 2 Solubilities in the quaternary system NaBr–KBr–$CaBr_2$–H_2O at 348.15 K

No.	Composition of solution, w (%)[a]			Composition of dry salt J (g/100 g.S) J (NaBr + KBr + $CaBr_2$) = 100 g				Equilibrium solid
	NaBr	KBr	$CaBr_2$	NaBr	KBr	$CaBr_2$	H_2O	
1, A_2	48.23	11.83	0.00	80.30	19.70	0.00	66.50	NaBr + KBr
2	45.08	10.71	4.73	74.49	17.70	7.82	65.23	NaBr + KBr
3	43.53	10.30	6.46	72.20	17.08	10.71	65.86	NaBr + KBr
4	40.93	9.83	10.46	66.86	16.06	17.09	63.35	NaBr + KBr
5	32.23	7.71	26.26	48.69	11.65	39.67	51.06	NaBr + KBr
6	28.63	6.81	32.07	42.41	10.09	47.50	48.13	NaBr + KBr
7	24.27	6.28	39.19	34.80	9.00	56.19	43.39	NaBr + KBr
8	23.11	6.04	41.21	32.85	8.58	58.57	42.13	NaBr + KBr
9	17.39	5.19	47.24	24.91	7.43	67.66	43.23	NaBr + KBr
10	13.70	4.83	53.40	19.05	6.71	74.24	39.02	NaBr + KBr
11, E_2	9.29	4.21	57.08	13.16	5.96	80.87	41.68	NaBr + KBr + $CaBr_2 \cdot 2H_2O$
12	7.46	3.15	59.84	10.59	4.47	84.94	41.94	NaBr + $CaBr_2 \cdot 2H_2O$
13	5.76	2.38	62.43	8.16	3.37	88.47	41.70	NaBr + $CaBr_2 \cdot 2H_2O$
14, B_2	4.58	0.00	67.84	6.32	0.00	93.68	38.08	NaBr + $CaBr_2 \cdot 2H_2O$
15	3.59	1.50	19.72	14.47	6.05	79.48	303.06	KBr + $CaBr_2 \cdot 2H_2O$
16	3.43	2.21	30.12	9.59	6.18	84.23	179.64	KBr + $CaBr_2 \cdot 2H_2O$
17	3.35	2.52	35.32	8.13	6.12	85.75	142.78	KBr + $CaBr_2 \cdot 2H_2O$
18	2.48	2.63	37.19	5.86	6.22	87.92	136.41	KBr + $CaBr_2 \cdot 2H_2O$
19	1.95	2.71	38.46	4.52	6.28	89.19	131.91	KBr + $CaBr_2 \cdot 2H_2O$
20	1.58	3.01	43.01	3.32	6.32	90.36	110.08	KBr + $CaBr_2 \cdot 2H_2O$
21, C_2	0.00	4.70	68.34	0.00	6.43	93.57	36.91	KBr + $CaBr_2 \cdot 2H_2O$

[a] w (%): mass%

fractions w, J is the Janeäcke index, with $J(\mathrm{KBr}) + J(\mathrm{NaBr}) + J(\mathrm{CaBr_2}) = 100$ g. Based on the data in Table 2, a stable equilibrium phase diagram of the system at 348.15 K is given in Fig. 3.

The quaternary system KBr–NaBr–$CaBr_2$–H_2O at 348.15 K has no complex salt or solid solution. There is one invariant point, three univariant curves, and three regions of crystallization in this system. The three crystallization fields corresponding to KBr, NaBr and $CaBr_2 \cdot 2H_2O$. The crystallization area of potassium bromide (KBr) is larger than that of other salts. This means that KBr has a lower solubility than the other salts in the quaternary NaBr–KBr–$CaBr_2$–H_2O system.

Three univariant curves are A_2E_2, B_2E_2, and C_2E_2. Point E_2 is the invariant point for the system KBr–NaBr–$CaBr_2$–H_2O at 348.15 K, which is saturated with KBr, NaBr, and $CaBr_2 \cdot 2H_2O$, and the composition of the corresponding liquid phase is w (KBr) = 0.0421, w (NaBr) = 0.0929, and w ($CaBr_2$) = 0.5708.

Figure 4 shows the water content diagram of the quaternary system KBr–NaBr–$CaBr_2$–H_2O at 348.15 K, and the abscissa is the Jänecke index values of KBr. Figure 4 shows that the water content increases at the univariant curves E_2C_2, and remains unchanged at the univariant curves A_2E_2 and B_2E_2 with an increase of the Jänecke index values of J (KBr). It reaches its biggest value at the point C_2.

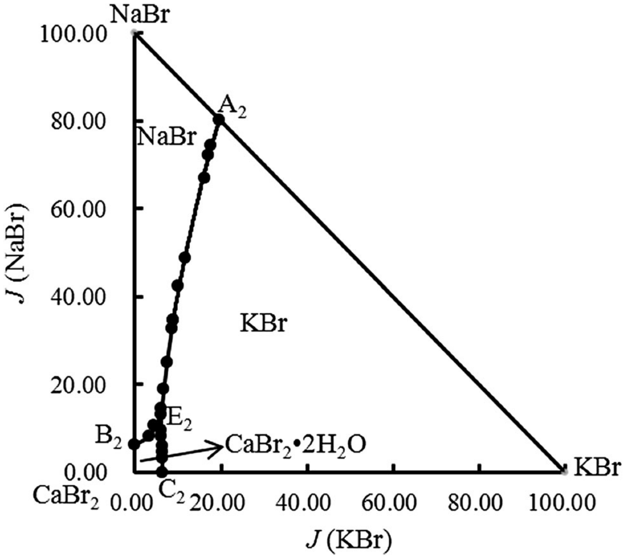

Fig. 3 Dry-salt solubility diagram of quaternary system NaBr–KBr–$CaBr_2$–H_2O at 348.15 K

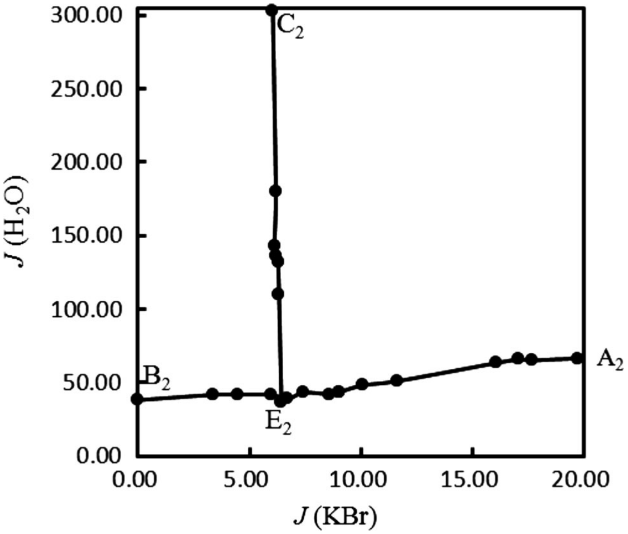

Fig. 4 Water contents of saturated solutions in the quaternary system NaBr–KBr–$CaBr_2$–H_2O at 348.15 K

4 Solubility Predictions

4.1 Model Parametrization

Pabalan [26] proposed a high temperature thermodynamic model for the concentrated electrolyte solution system Na–K–Mg–Ca–SO_4–OH–H_2O over a temperature range (from

273.15 to 473.15 K). In order to obtain thermodynamic properties and parameters of the ternary solutions, such as osmotic coefficients ϕ, binary and ternary ionic interaction parameters, and dissolution equilibrium constant K, the following equations were applied to the phase equilibria and chemical equilibria of a given solution [27]:

$$\mathrm{Par}(T) = a_1 + a_2T + a_5T^{-1} + a_6 lnT \tag{1}$$

$$K(\mathrm{KBr}) = \gamma_{\pm}^2 m^2 \tag{2}$$

$$K(\mathrm{NaBr}) = \gamma_{\pm}^2 m^2 \tag{3}$$

$$K(\mathrm{MgBr_2 \cdot 6H_2O}) = 4\gamma_{\pm}^3 m^3 a_{\mathrm{w}}^6 \tag{4}$$

$$K(\mathrm{CaBr_2 \cdot 2H_2O}) = 4\gamma_{\pm}^3 m^3 a_{\mathrm{w}}^2 \tag{5}$$

$$K(\mathrm{KBr \cdot MgBr_2 \cdot 6H_2O}) = \mathrm{m_{K^+}} \cdot \gamma_{\mathrm{K^+}} \cdot \mathrm{m_{Mg^{2+}}} \cdot (\mathrm{m_{Br^-}} \cdot \gamma_{\mathrm{Br^-}})^3 \cdot \mathrm{a_w^6} \tag{6}$$

where Par(T) refers to temperature functions for the model parameters as described in Møller (1988); the temperature T is in Kelvin. The Debye–Hückel constant A^{ϕ} was taken from the literature [28]. The parameters a_1, a_2, a_5 and a_6 are based on the results of Christov [20]. In Eqs. 2–5, γ_i and m_i are the activity coefficient and molality of solute species i, respectively.

4.2 Solubility Calculation

Based on Pitzer's ion-interaction model for aqueous electrolyte solutions and the corresponding temperature-dependent parameter expressions, the dissolution equilibrium constant (K) of solid salts ($MgBr_2 \cdot 6H_2O$, $KBr \cdot MgBr_2 \cdot 6H_2O$, NaBr, KBr and $CaBr_2 \cdot 2H_2O$) were fitted by multiple linear regression method. The constants in Eq. 1 for the binary and ternary interaction parameters are taken from the literature [20] (see Table 3). Table 4 shows the calculated dissolution equilibrium constant (ln K) values at 348.15 K.

Harvie and Weare [6] showed that the Pitzer approach could be extended to accurately calculate salt solubilities in complex brines. The solubilities of salts in two quaternary systems at 348.15 K were calculated with the Pitzer model. As shown in Figs. 5 and 6, the experimental and predicted phase diagrams (dashed line) of the two quaternary systems at 348.15 K are in general agreement. Tables 5 and 6 give a comparison of the calculated and experimental solubilities at the invariant points of the two quaternary systems and the saturated solution compositions of the relevant quaternary subsystems, respectively. As can be seen from Figs. 5 and 6, there are some deviations between the calculated and experimental solubilities. The sources of deviations include (1) experimental uncertainty, and (2) uncertainties of the ion-interaction parameters of Pitzer's equation due to the regression and the experimental data used in the regression, although the regression equation is applicable only in a certain temperature range (the accuracy of the ion-interaction model requires further validation at high temperatures and high concentrations). Overall, the above results indicate that the model used in this work is capable of a reasonable prediction of the salt solubilities for the quaternary systems in question.

Table 3 Binary and ternary interaction parameters in Eq. 1

Parameters	Constants (temperature in degrees Kelvin)			a_6 (ln$T$)	Refs.
	a_1	a_2 (T)	a_5 ($1/T$)		
$\beta^{(0)}_{\mathrm{NaBr}}$ (273.15–573.15 K)	$7.11600256 \times 10^{-1}$	$-7.51986135 \times 10^{-4}$	$-1.09266366 \times 10^{2}$	0	[20]
$\beta^{(1)}_{\mathrm{NaBr}}$ (273.15–573.15 K)	-4.97335195	$8.57795255 \times 10^{-3}$	7.38610135×10^{2}	0	[20]
C^{ϕ}_{NaBr} (273.1–573.15 K)	$-7.34172496 \times 10^{-2}$	$8.71449532 \times 10^{-5}$	1.33019597×10	0	[20]
$\beta^{(0)}_{\mathrm{KBr}}$ (273.15–573.15 K)	$4.79896100 \times 10^{-1}$	$-4.17396303 \times 10^{-4}$	-9.05196847×10	0	[20]
$\beta^{(1)}_{\mathrm{KBr}}$ (273.15–73.15 K)	-4.13092017	$6.85308052 \times 10^{-3}$	7.04957954×10^{2}	0	[20]
C^{ϕ}_{KBr} (273.15–573.15 K)	$-5.93226684 \times 10^{-2}$	$6.33899074 \times 10^{-5}$	1.17934031×10	0	[20]
$\beta^{(0)}_{\mathrm{MgBr_2}}$(273.15–438.15 K)	7.14660368	$-1.02197350 \times 10^{-2}$	$-1.09274058 \times 10^{3}$	0	[20]
$\beta^{(1)}_{\mathrm{MgBr_2}}$(273.15–438.15 K)	-6.26940853×10	$9.95433504 \times 10^{-2}$	1.03606736×10^{4}	0	[20]
$C^{\phi}_{\mathrm{MgBr_2}}$ (273.15–438.15 K)	$-4.20446793 \times 10^{-1}$	5.9813951×10^{-4}	7.29856800×10	0	[20]
$\beta^{(0)}_{\mathrm{CaBr_2}}$ (273.15–438.15 K)	1.93796297	$-2.02463996 \times 10^{-3}$	$-2.97733495 \times 10^{2}$	0	[20]
$\beta^{(1)}_{\mathrm{CaBr_2}}$ (273.15–523.15 K)	-5.32419836×10	$7.54397694 \times 10^{-2}$	1.00344685×10^{4}	0	[20]
$C^{\phi}_{\mathrm{CaBr_2}}$ (273.15–523.15 K)	$-2.49439694 \times 10^{-1}$	$2.61696289 \times 10^{-4}$	5.37832428×10	0	[20]
$\theta_{\mathrm{Na,K}}$ (273.15–523.15 K)	$-5.02312111 \times 10^{-2}$	0	1.40213141×10	0	[20, 21]
$\psi_{\mathrm{Na,K,Br}}$ (273.15–348.15 K)	$-1.73305922 \times 10^{-2}$	$3.50504594 \times 10^{-5}$	1.28020967	0	[20, 21]
$\theta_{\mathrm{K,Mg}}$ (273.15–473.15 K)	0	0	0	0	[20, 22]
$\psi_{\mathrm{K,Mg,Br}}$ (273.15 –323.15 K)	6.05037096×10	$1.78735421 \times 10^{-2}$	$-1.55748662 \times 10^{3}$	-1.06419353×10	[20, 22]
$\theta_{\mathrm{Na.Mg}}$ (273.15 –473.15 K)	0.07	0	0	0	[20, 23]
$\psi_{\mathrm{Na,Mg,Br}}$ (273.15–373.15 K)	$1.69940176 \times 10^{-1}$	0	-4.93791545×10	0	[20, 23]
$\theta_{\mathrm{K,Ca}}$ (273.15 –523.15 K)	1.156×10^{-1}	0	0	0	[20]
$\psi_{\mathrm{K,Ca,Br}}$ (273.15–373.15 K)	-8.99914531×10	$-2.46230545 \times 10^{-2}$	2.42806168×10^{3}	1.56463896×10	[20]
$\theta_{\mathrm{Na,Ca}}$ (273.15–523.15 K)	5.00×10^{-2}	0	0	0	[20]
$\psi_{\mathrm{Na,Ca,Br}}$ (273.15–373.15 K)	6.06567329×10	$1.79115831 \times 10^{-2}$	$-1.56036933 \times 10^{3}$	-1.06670101×10	[20]

Table 4 Dissolution equilibrium constant of salts (*K*) at 348.15 K calculated in this work

Salts	NaBr	KBr	$CaBr_2 \cdot 2H_2O$	$MgBr_2 \cdot 6H_2O$	$KBr \cdot MgBr_2 \cdot 6H_2O$
lnK	6.414	3.457	17.298	12.069	15.951
Ref.	This work	This work	This work	This work	This work

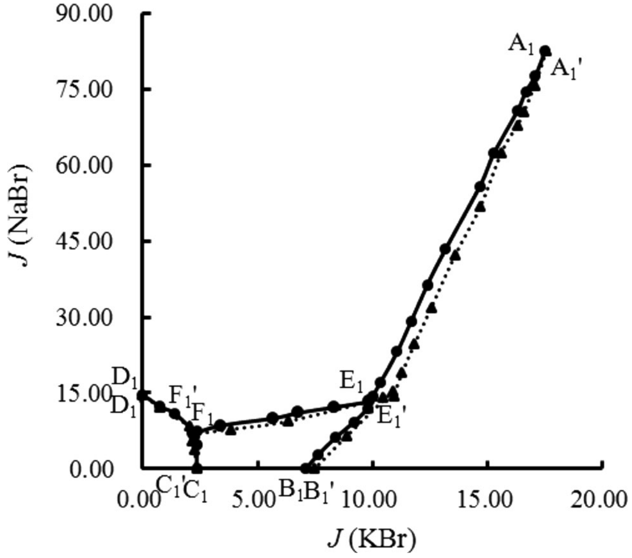

Fig. 5 Comparison of calculated and experimental solubilities of salts in the $KBr–NaBr–MgBr_2–H_2O$ system at 348.15 K: experimental (*filled circle*); calculated (*filled triangle*)

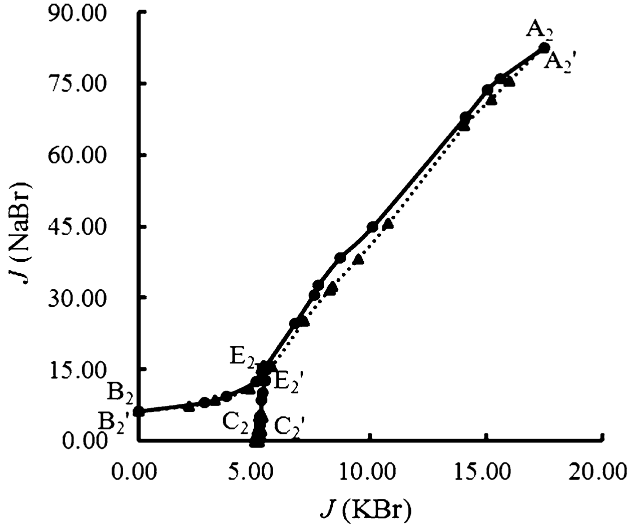

Fig. 6 Comparison of calculated and experimental solubilities of salts in the quaternary system $KBr–NaBr–CaBr_2–H_2O$ at 348.15 K: experimental (*filled circle*); calculated (*filled triangle*)

Table 5 Comparison of experimental and calculated invariant points of the quaternary system KBr–NaBr–$MgBr_2$–H_2O and its binary subsystems at 348.15 K

No.	Composition of solution, *w* (%)			Equilibrium solid phase
	NaBr	KBr	$MgBr_2$	
A_1	48.23	11.83	0.00	NaBr + KBr
A_1'	48.21	11.79	0.00	NaBr + KBr
B_1	0.00	4.17	40.43	KBr + $KBr{\cdot}MgBr_2{\cdot}6H_2O$
B_1'	0.00	3.87	38.23	KBr + $KBr{\cdot}MgBr_2{\cdot}6H_2O$
C_1	0.00	1.62	52.27	$KBr{\cdot}MgBr_2{\cdot}6H_2O$ + $MgBr_2{\cdot}6H_2O$
C_1'	0.00	1.58	52.26	$KBr{\cdot}MgBr_2{\cdot}6H_2O$ + $MgBr_2{\cdot}6H_2O$
D_1	9.28	0.00	48.21	NaBr + $MgBr_2{\cdot}6H_2O$
D_1'	9.24	0.00	48.13	NaBr + $MgBr_2{\cdot}6H_2O$
F_1	3.11	1.46	43.30	NaBr + $MgBr_2{\cdot}6H_2O$ + $KBr{\cdot}MgBr_2{\cdot}6H_2O$
F_1'	3.09	1.43	43.32	NaBr + $MgBr_2{\cdot}6H_2O$ + $KBr{\cdot}MgBr_2{\cdot}6H_2O$
E_1	7.22	5.93	30.77	NaBr + KBr + $KBr{\cdot}MgBr_2{\cdot}6H_2O$
E_1'	7.18	5.89	30.75	NaBr + KBr + $KBr{\cdot}MgBr_2{\cdot}6H_2O$

A_1–F_2: experimental results; A_1'–F_1': calculated results

Table 6 Comparison of experimental and calculated invariant points of the quaternary system KBr–NaBr–$CaBr_2$–H_2O and its binary subsystems at 348.15 K

No.	Composition of solution, *w* (%)			Equilibrium solid phase
	NaBr	KBr	$CaBr_2$	
A_2	48.23	11.83	0.00	NaBr + KBr
A_2'	48.21	11.79	0.00	NaBr + KBr
B_2	4.58	0.00	67.84	NaBr + $CaBr_2{\cdot}2H_2O$
B_2'	4.46	0.00	67.81	NaBr + $CaBr_2{\cdot}2H_2O$
C_2	0.00	4.70	68.34	KBr + $CaBr_2{\cdot}2H_2O$
C_2'	0.00	4.61	68.23	KBr + $CaBr_2{\cdot}2H_2O$
E_2	9.29	4.21	57.08	NaBr + KBr + $CaBr_2{\cdot}6H_2O$
E_2'	9.25	3.97	57.04	NaBr + KBr + $CaBr_2{\cdot}6H_2O$

A_2–E_2: experimental results; A_2'–E_2': calculated results

5 Conclusion

The solubilities of salts in the systems KBr–NaBr–$MgBr_2$–H_2O and KBr–NaBr–$CaBr_2$–H_2O at 348.15 K were determined with the method of isothermal solution saturation. According to the experimental data, the stable equilibrium phase diagrams and water content diagrams of the two quaternary systems were constructed. Based on Pitzer's model and temperature-dependent parameter expressions, the dissolution equilibrium constant of the salts are represented. The solubilities of salts in the quaternary systems were predicted at 348.15 K. The results indicate that the Pitzer model based on the temperature-dependent parameter expressions is applicable for the prediction of solubilities in the quaternary systems.

Acknowledgments This project was supported by the National Natural Science Foundation of China (41373062, U1407108), the Specialized Research Fund (20125122110015) for the Doctoral Program of Higher Education of China, and the Scientific Research and Innovation Team in Universities of Sichuan Provincial Department of Education (15TD0009).

References

1. Sun, B., Li, B., Fang, C.H., Du, X.H., Song, P.S.: Lithium salt lake brine system related research. J. Salt Lake Res. **3**, 34–39 (1995). **(in Chinese)**
2. Zhang, Z.L., Sang, S.H., Li, M.: Study on metastable phase equilibrium of quaternary system $K_2B_4O_7$–K_2SO_4–KCl–H_2O at 298 K. Chem. Eng. **5**, 46–48 (2009). **(in Chinese)**
3. Shu, S.B., Xu, Y.L., Xu, E.X., Xiao, C.W.: Study on the occurrence of potassium-rich brine in a geological structure in West Sichuan and the analytical patterns. Chin. Well Rock Salt **2**, 2–26 (2003). **(in Chinese)**
4. Lin, Y.T., Cao, S.X.: New discovery rare gas field with rich potassium and boron in West Sichuan Basin. Chin. Geogr. **7**, 45–47 (2001). **(in Chinese)**
5. Harvie, C.E., Weare, J.H., Hardie, L.A., Eugster, H.P.: Evaporation of seawater: calculated mineral sequences. Science **208**, 498–500 (1980)
6. Harvie, C.E., Weare, J.H.: The prediction of mineral solubilities in natural waters: the Na–K–Mg–Ca–Cl–SO_4–H_2O system from zero to high concentration at 25 °C. Geochim. Cosmochim. Acta **44**, 981–997 (1980)
7. Harvie, C.E., Eugster, H.P., Weare, J.H.: Mineral equilibriain the six-component seawater system, Na–K–Mg–Ca–SO_4–Cl–H_2O at 25 °C. II: compositions of the saturated solutions. Geochim. Cosmochim. Acta **46**, 1603–1618 (1982)
8. Harvie, C.E., Møller, N., Weare, J.H.: The prediction of mineral solubilities in natural waters: the Na–K–Mg–Ca–H–Cl–SO_4–OH–HCO_3–CO_3–CO_2–H_2O system from zero to high concentration at 25 °C. Geochim. Cosmochim. Acta **48**, 723–751 (1984)
9. Felmy, A.R., Weare, J.H.: The prediction of borate mineral equilibria in natural waters: application to Searles Lake. California. Geochim. Cosmochim. Acta **50**, 2771–2783 (1986)
10. Weng, Y.B., Wang, J.K., Yin, Q.X., Wang, Y.F.: Phase diagram for the ternary system of K^+/Cl^-, Br^-–H_2O at 298 K, 313 K and 333 K. Petrochem. Technol. **4**, 358–361 (2007). **(in Chinese)**
11. Zhang, K.J., Sang, S.H., Wang, D., Zhang, J.J.: Phase equilibrium in the ternary system KCl–KBr–H_2O at 323 K. J. Salt Chem. Ind. **6**, 5–7 (2011). **(in Chinese)**
12. Hu, Y.X., Sang, S.H., Cui, R.Z., Zhong, S.Y.: Phase equilibrium in the ternary system KCl–KBr–H_2O at 373 K. Chin. Sci. Pap. **9**, 847–850 (2013). **(in Chinese)**
13. Tang, Z.X., Zhang, F.X., Guo, Z.Z., Huang, J.Y.: Potassium lithium halide water system research. IV. The solubilities of ternary systems NH_4I–LiI–H_2O, LiI–LiBr–H_2O and NH_4Br–LiBr–H_2O 298 K. J. Salt Lake Res. **3**, 9–13 (1993)
14. Sang, S.H., Yin, H.A., Ni, S.J., Zhang, C.J.: A study on equilibrium solubilities and properties of solutions in the ternary system $K_2B_4O_7$–KBr–H_2O at 298 K. J. Chengdu Univ. Techol Ed. **4**, 414–416 (2006) (**in Chinese**)
15. Sang, S.H., Yu, H.Y.: Study on the phase equilibrium of $Na_2B_4O_7$–NaBr–H_2O ternary system at 298 K. Sea Lake Salt Chem. Ind. **2**, 4–5 (2006). **(in Chinese)**
16. Sang, S.H., Sun, L.M., Li, H., Zhang, X., Zhang, K.J.: Study on phase equilibria for quaternary system of Na^+, K^+/Br^-, SO_4^{2-}–H_2O at 323 K. Chin. J. Inorg. Chem. **5**, 845–849 (2011) (**in Chinese**)
17. Zhang, Y.G., Sang, S.H., Zhang, K.J., Hu, F.M., Cui, R.Z.: Study on phase equilibria for quaternary system of NaCl–NaBr–Na_2SO_4–H_2O at 348 K. J. Salt Chem. Ind. **2**, 12–15 (2013). **(in Chinese)**
18. Ning, H.Y., Sang, S.H., Wang, D., Zeng, X.X.: Study on phase equilibria in $Na_2B_4O_7$–NaBr– Na_2SO_4–H_2O quaternary system at 348 K. Chem. Eng. **4**, 27–30 (2012). **(in Chinese)**
19. Wang, D., Sang, S.H., Zeng, X.X., Ning, H.Y.: Phase equilibrium of KCl–KBr–K_2SO_4–H_2O quaternary system at 323 K. Petrochem. Techol. **3**, 285–288 (2011). **(in Chinese)**
20. Christov, C.: Study of bromide salts solubility in the (m1KBr + m2$CaBr_2$)(aq) system at $T = 323.15$ K. Thermodynamic model of solution behavior and (solid + liquid) equilibria in the ternaries (m1KBr + m2$CaBr_2$)(aq), and (m1$MgBr_2$ + m2$CaBr_2$)(aq), and in the quinary (Na + K + Mg + Ca + Br + H_2O) systems to high concentration and temperature. J. Chem. Thermodyn. **55**, 7–22 (2012)
21. Christov, C.: An isopiestic study of aqueous NaBr and KBr at 50 °C: chemical equilibrium model of solution behavior and solubility in the NaBr–H_2O, KBr–H_2O and Na–K–Br–H_2O systems to high concentration and temperature. Geochim. Cosmochim. Acta **71**, 3557–3569 (2007)
22. Christov, C.: Isopiestic investigation of the osmotic coefficients of $MgBr_2$(aq) and study of bromide salts solubility in the (m1KBr + m2MgBr2)(aq) system at $T = 323.15$ K. Thermodynamic model of solution behaviour and (solid + liquid) equilibria in the $MgBr_2$(aq), and (m1KBr + m2MgBr2)(aq) systems to high concentration and temperature. J. Chem. Thermodyn. **43**, 344–353 (2011)
23. Christov, C.: Study of bromide salts solubility in the (m1NaBr + m2$MgBr_2$)(aq) system at 323.15 K. Thermodynamic model of solution behavior and (solid–liquid) equilibria in the (Na + K +

Mg + Br + H_2O) system to high concentration and temperature. J. Chem. Thermodyn. **47**, 335–340 (2012)

24. Christov, C.: Isopiestic investigation of the osmotic coefficients of aqueous $CaBr_2$ and study of bromide salt solubility in the $NaBr–CaBr_2–H_2O$ system at 50 °C: thermodynamic model of solution behavior and solid–liquid equilibria in the $CaBr_2–H_2O$, and $NaBr–CaBr_2–H_2O$ systems to high concentration and temperature. CALPHAD **35**, 42–53 (2011)
25. Institute of Qinghai Salt-Lakes, Chinese Academy of Sciences: Analytical Methods of Brines and Salts, 2nd edn. Science Press, Beijing (1988). **(in Chinese)**
26. Pabalan, R., Pitzer, K.S.: Thermodynamics of concentrate electrolyte mixtures and the prediction of mineral solubilities to high temperatures for mixtures in the system Na–K–Mg–Cl–SO_4–OH–H_2O. Geochim. Cosmochim. Acta **51**, 2429–2443 (1987)
27. Christov, C., Møller, N.: Chemical equilibrium model of solution behavior and solubility in the H–Na–K–OH–Cl–HSO_4–SO_4–H_2O system to high concentration and temperature. Geochim. Cosmochim. Acta **68**, 1309–1331 (2004)
28. Ananthaswamyt, J., Atklnson, G.: Thermodynamics of concentrated electrolyte mixtures: 4. Pitzer–Debye–Hückel limiting slopes for water from 0 to 100 °C and from 1 atm to 1 kbar. J. Chem. Eng. Data **29**, 81–87 (1984)